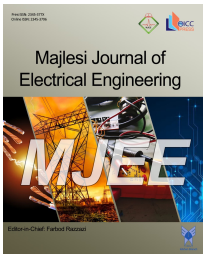

Volume 18, Issue 3, 182440 (1-16)

Majlesi Journal of Electrical Engineering (MJEE)

https://doi.org/10.57647/j.mjee.2024.180340

Grey Wolf Optimized PID controller to control the frequency in a five-area power system in the presence of uncertainties

Narender Saini*, Jyoti Ohri

National Institute of Technology Kurukshetra, Kurukshetra, India.

***Corresponding author:** narender_61900104@nitkkr.ac.in

Original Research

Received:
10 April 2024
Revised:
20 June 2024
Accepted:
2 July 2024
Published online:
30 September 2024

Abstract:

Providing reliable and sufficient power to the client is essential. Power quality is determined by the consistency of frequency and tie-line power between control regions. Thus, the importance of Load Frequency Control in an electrical network cannot be overstated. In this work, a PID controller using the Grey Wolf Optimization algorithm is employed to help with frequency management in a multi-area power network. A reheated turbine power system with five area is controlled by the PID controller. The experimental data showed a comparison between GWO-PID, Genetic Algorithm-based PID, Particle Swarm Optimization-based PID, and Firefly Algorithm-based PID. With a 1 % step load variation, the findings confirmed the efficiency of using the integral time absolute error (*ITAE*) performance index. GA, PSO, and FA can't keep up with the GWO-based PID controller when it comes to optimising an integrated power system. Simulation results reveal that GWO has the shortest settling time for frequency variations, as well as the lowest undershoot, overshoot, and *ITAE* values. To evaluate the robustness of GWO-PID, sensitivity analysis is done by modifying the system parameters like turbine and governor time constant in the range of $\pm 10\,\%$ from their nominal values.

Keywords: Frequency control; Frequency fluctuations; Five-area power system; PID controller; Grey Wolf Optimization

1. Introduction

The electrical system is a vast network including several linked systems. An interconnected electrical power system aims to generate, transfer, and distribute electrical energy at the most efficient frequency and voltage for the system's functioning. The theory governing the regulation of power systems states that the system's frequency is controlled by the produced real power, while the generated reactive power controls the terminal voltage. The power system's instability arises from a discrepancy between the power generated and the power demanded by the load. This results in the frequency deviating from the anticipated value. The primary goal of Load Frequency Control (LFC) is to maintain frequency stability by minimizing frequency deviations to zero. This is achieved by regulating two control loops to maintain the precise balance between the generated and required power.

Primary frequency control refers to the regulation of the frequency of an electrical power system within a narrow range of acceptable values. The operational time restrictions for the main frequency control range from 2 to 20 seconds. Major components include the inertial response, which is alternatively referred to as the fast response, and the governor's response was described as sluggish.
Secondary/supplementary frequency control refers to the additional measures used to regulate and maintain the frequency of a system, commonly referred to as AGC or LFC. The duration of its operation ranges from 20 seconds to 2 minutes. When there is a discrepancy between the demand for power and the amount of power being produced, it assists in stabilizing the system's frequency and controlling the transfer of electricity across linked regions [1].
Various controllers and techniques have been designed for the LFC issue over the last few years, but some improvement is still needed. The idea of advanced optimum control

was initially presented in [2] for the AGC of the multi-area power system. A comprehensive examination of the recent advancements and execution of diverse control strategies pertaining to frequency and power regulation in AGC systems is detailed in [3], and [4]. The load frequency control problem for single-area [5] and multi-area power systems are discussed in [6]. A fuzzy classical controller is proposed to enhance the performance of two-area electrical power systems. The controller incorporates an output scaling factor for improved control. A version of the imperialist competitive algorithm (ICA) optimizes the output scaling factor of a fuzzy proportional integral controller using the integral squared error criteria [7].
In [8], the LFC of three areas with reheat turbine and GRC effect is presented. PID as a supplementary controller is suggested for a five-area reheated thermal power plant [9]. In [10–12], the sliding mode controller regulates frequency variations in microgrid and multi-area power systems, including hydro and thermal units. Other kinds of controllers such as Fuzzy classical controller [13], PD+PID cascaded controller [14], PID controller [9, 15–17], Fractional order (FO) PID [18], Model Predictive Control (MPC) [19–21] is commonly used in the AGC as a secondary/supplementary control to keep the frequency stable. In [22], a hybrid controller called FOPI minus FOPD with a filter coefficient is utilised to enhance AGC.
Research on LFC controllers found that performance was entirely dependent on the values chosen for controller parameter settings in virtually all trials that employed conventional controllers. The best gain value for each controller must be determined in order to improve controller performance. Controller tuning has traditionally been achieved through hit-and-trial procedures, such as ZN and similar ones. These approaches are ineffective because of the electrical network's dynamic load demand and many non-linearities.
As a result of this, we will be required to implement new procedures, as well as heuristic and meta-heuristic approaches, that are more efficient such as Teaching Learning Based Optimization (TLBO) [8], Levenberg-Marquardt algorithm [23], Genetic Algorithm (GA) [24, 25], Bat algorithm (BA) [14], Particle Swarm Optimization (PSO) [26–28], crow-search algorithm [29], Backtracking Search Optimization Algorithm (BSA) [9], Ant-Lion Optimizer (ALO) [30], Salp Swarm Optimization (SSO) [31], Genetic Algorithm (GA) [24, 25], Differential Evolution (DE), Crow Search Algorithm [22], Imperialist Competitive Algorithm (ICA) [15, 20], Firefly Algorithm (FA) [9], and Artificial Bee Colony (ABC) [32], and Optimization, Ziegler-Nichols, fuzzy logic etc.

1.1 Previous work's motivation and limitation

Many optimization algorithms rely on the proper selection of different control parameters to be successful. The PSO algorithm's performance is influenced by the control parameters, including the inertia weights (W_1 and W_2), the social factors (C_1), and the cognitive parameters (C_2). The performance of the DE algorithm is influenced by two control parameters: the crossover rate (CR) and the scaling factor (F). Three distinct variables affect FA: α, β, and γ. The choice of these parameters is crucial for determining the success of the algorithms. According to the "no free lunch" theory, no optimization strategy exists that applies to all sorts of optimization problems. This prompts us to propose an enhanced technique that strictly regulates parameters without any external control, aiming to resolve a wide range of unaddressed issues. To enhance the overall stability of the power system, it is justified to introduce a new optimization approach to examine the performance of Load Frequency Control (LFC). The GWO [28] the algorithm does not need any regulatory parameters. Researchers are inclined to use this approach in their respective fields of study since it is straightforward, efficient, and fast, owing to the algorithm's lack of necessary parameters.
Utilising PID controllers may enhance system performance. PID controllers have achieved significant success due to several factors: the availability of effective tuning rules, a straightforward transfer function, and industrial adoption requiring minimal process expertise. Enhancing control is a primary objective in control engineering since it paves the way for developing more effective control algorithms. Therefore, in this study, is used. Assessing the controller's gain might be challenging due to its crucial role in determining efficiency. Various methodologies are used to compute the optimal possible gain value since this is an optimization issue. The GWO method evaluates the controller's ability to manage frequency fluctuations in a five-area power system. According to the simulation findings, the GWO-optimized PID controller surpasses the other optimization techniques in every manner. Finally, the robustness of the GWO-PID is investigated in the presence of uncertainties, by modifying the system's characteristics, such as the turbine and governor time constants, both by up to 10 %.

1.2 Contribution and novelty

The research paper proposes Grey Wolf Optimized PID controller to control the frequency and power flow through tie-lines in a five-area power system in the presence of uncertainties. The research paper presents several novel contributions that distinguish it from previous works. These are:

1. Application of Grey Wolf Optimized algorithm to design a PID controller for regulating the frequency in a complex five-area single unit power system. The selection of a five-area power system for LFC aims to provide a practical and demanding environment for assessing control techniques and enhancing the stability and reliability of the power system.
2. Comparison of the GWO-PID controller's performance with other existing controllers, including PSO-PID, FA-PID, and GA-PID controllers.
3. Analysis of the robustness of the GWO-PID controller under load variations and parameter's uncertainties.
4. Validation of the proposed controller using simulation studies in MATLAB/Simulink, demonstrating its efficacy and potential for practical application.

The rest of the research is broken out as follows: Modelling of the test system and controller is the subject of Section 2.

In the third section a concise review of the GWO algorithm. The results of simulations run using GWO, and comparison with other methodologies that were taken into consideration are shown in the next section. Section 5 discussed the robustness. In the end, the conclusion may be found in section 6.

2. Modeling of power system

2.1 Five-area power system model

The present study aims to analyze a five-area power system model, as indicated in Fig. 1. Each region in the considered model is equipped with a thermal power system that consists of a governor, reheat turbine, and turbine unit. Transfer function of each unit are used in the model for simulation process. A governor, also called a primary controller, is a device used to measure and control the speed by controlling the valve position and, by doing so, control the frequency. Its transfer function is given by [1]:

$$\mathrm{T_G}(s) = \frac{1}{1+s\mathrm{T_{Gi}}} \tag{1}$$

The primary function of the turbine is to convert the energy derived from steam into mechanical energy, which in turn drives the rotation of the generator. Its transfer function is [1]:

$$\mathrm{T_T}(s) = \frac{1}{1+s\mathrm{T_{Ti}}} \tag{2}$$

Thermal power plants often use reheat turbines to improve the system's efficiency. These turbines raise the temperature of the steam just before it reaches the low-pressure turbine. Its transfer function is given by [33]:

$$\mathrm{T_r}(s) = \frac{1+sK_{\mathrm{ri}}\mathrm{T_{ri}}}{1+s\mathrm{T_{ri}}} \tag{3}$$

The overall transfer function of a power system having a load and generator is [33]:

$$\mathrm{T_{Ps}}(s) = \frac{K_{\mathrm{Pi}}}{1+s\mathrm{T_{Pi}}} \tag{4}$$

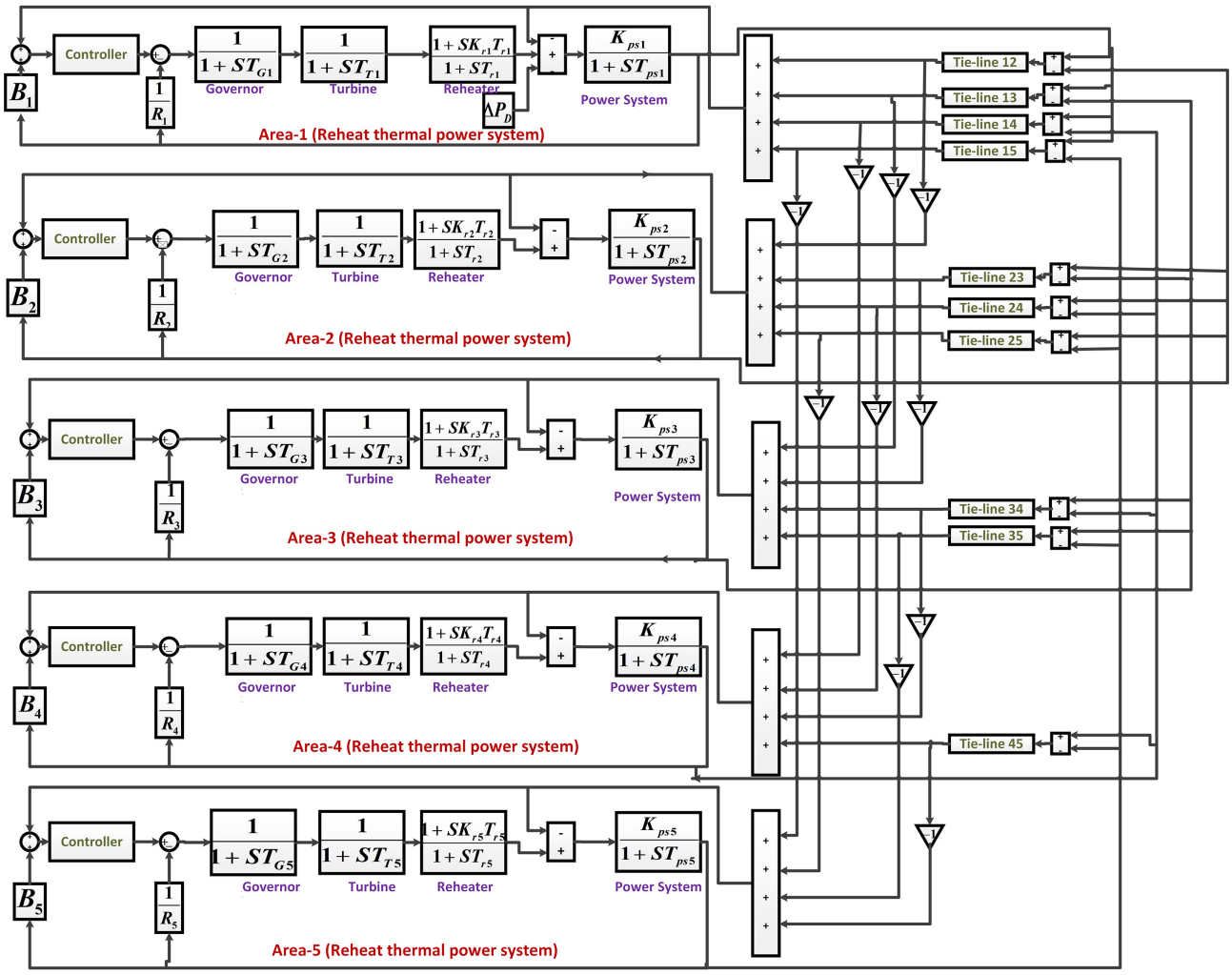

Figure 1. Five-area thermal power system.

where $i = 1,2,\ldots 5$. And,

$$K_{\mathrm{P}i} = \frac{1}{D_i} \tag{5}$$

$$\mathrm{T}_{\mathrm{P}i} = \frac{2\mathrm{H}_i}{fD_i} \tag{6}$$

The following is a definition of each symbol that is used by this system:
B_1 to $B_5 \rightarrow$ Frequency bias parameters in corresponding areas.
R_1 to $R_5 \rightarrow$ Speed regulation parameters (p.u.).
$\mathrm{T_{r1}}$ to $\mathrm{T_{r5}} \rightarrow$ Reheat turbine time constant (sec).
$\mathrm{T_{T1}}$ to $\mathrm{T_{T5}} \rightarrow$ Turbine time constant (sec).
ACE_1 to $ACE_5 \rightarrow$ Area control errors in corresponding area.
K_{r1} to $K_{\mathrm{r5}} \rightarrow$ Reheater gain.
$\mathrm{H} \rightarrow$ Inertia Constant.
$\Delta P_D \rightarrow$ Load change in Area-1.
$\mathrm{T_{G1}}$ to $\mathrm{T_{G5}} \rightarrow$ Governor time constants (sec).
$\mathrm{T_{P1}}$ to $\mathrm{T_{P5}} \rightarrow$ Power system's time constants.
K_{P1} to $K_{\mathrm{P5}} \rightarrow$ Power systems gain.
Δf_1 to $\Delta f_5 \rightarrow$ Frequency variations in corresponding areas.
$D \rightarrow$ Load damping coefficient.
$f \rightarrow$ Nominal frequency.
The parameters value for the tested system are taken from [9].
Tie lines link the five separate areas of an interconnected power system, allowing electricity to flow between them. Due to a little change in load, the output frequencies of all regions are impacted, and the tie line power flow is also affected. In order to re-establish the predetermined levels of tie line powers and area frequency, the control system of each area needs input from the transitory conditions of all other areas. The power deviation through tie-lines discovers information about the different regions, whereas each output frequency finds information about its own.
An input to the controller is the corresponding area's ACE, which consists of the incremental change in power flow through tie-line and the related control area frequency mismatch, and is described by:

$$ACE_j = B_j \Delta f_j + \Delta P_{\mathrm{tie}j} \tag{7}$$

where $j = 1,2,\ldots 5$.

2.2 Controller and objective

A controller is needed to maintain tie-line power exchange across connected regions and manage frequency deviations since power demand changes arbitrarily, thus a PID controller is used in each area to handle the aforementioned problem of frequency deviations. In a shorter amount of time, it helps to improve system performance by reducing peak undershoot and overshoot in the response. The PID controller's transfer function is:

$$\mathrm{T_{PID}} = K_{\mathrm{P}} + \frac{K_{\mathrm{I}}}{s} + K_D s \tag{8}$$

The controller input u_i is given by [28]:

$$u_i = ACE_i K_{\mathrm{P}i} + ACE_i \frac{K_{\mathrm{I}i}}{s} + ACE_i K_{Di} s \tag{9}$$

where $i = 1,2,\ldots 5$.
PID controllers are used to minimize tie-line power deviations and frequency errors to zero as quickly as possible following an unanticipated increase or decrease in demand for power. Because gains are so crucial to the effectiveness of the PID controller, it may be challenging to calculate the controller's gain. The use of hit-and-trial approaches, such as ZN and other methods of a similar kind, often accomplished controller tuning. However, these methods are inefficient as a result of the ever-changing load demand and the many non-linearities present in the electrical network. Furthermore, in this work, the GWO technique is employed to discover the optimal parameters of PID controller. Because of this, the controller was able to reset ACE whenever a rapid shift in load disrupted the regions it was monitoring. The selection of an appropriate goal function is the single most crucial factor in the design of excellent controllers. The objective function chosen in this work is the *ITAE* Performance Index. The following is the *ITAE* formulation that takes into account frequency and tie-line power changes.

$$P.I = ITAE = \int_0^{t_s} \sum_{p=1}^{5} (|\Delta f_p| + |\Delta P_{\mathrm{tie}p}| dt) \tag{10}$$

3. Grey Wolf Optimization

Mirjalili et al. in 2014 proposed GWO as a meta-heuristic method for determining the social hierarchy and hunting habits of grey wolves in nature. They are considered the most powerful carnivores in the food chain. The majority of grey wolves prefer to live in packs (packs). Each pack has between 6 and 14 members on average. Each member of the team has a clearly defined place in the social order of responsibility.
There are four tiers of wolves in the social hierarchy. The first level is Alpha (α). They are in charge of making all of the choices for the pack. Beta (β) is the next stage. They are the wolves that take orders from the pack leader. The level that comes after this one is called Delta (δ), and although they are required to obey and, they are in charge of omega. The fourth and final level is called Omega (ω) since it is the lowest level. Following the alpha, beta, and delta rules is required of them. [14]. As the grey wolf stalks and pursues the target, harassing and encircling it until the prey is no longer moving, it attacks the victim. Once the target's location has been determined, the remaining wolves re-arrange their dens in accordance with the best search agents' placements.

3.1 Mathematical model of GWO algorithm

The fittest solution is alpha, followed by beta, and finally, delta in the GWO. Omega is the name for the rest of them. α, β, and δ generally direct the hunting process in the GWO algorithm, and ω have to be followed these three wolves. Following are the mathematical equations for encircling behavior:

$$D_P^{(i)} = |C_P \cdot P_{pq}^{*(i)} - P_{pq}^{(i)}| \tag{11}$$

$$P_{pq}^{(i+1)} = P_{pq}^{*(i)} - A_p \cdot D_q^i \tag{12}$$

where $p = 1, 2, \ldots N$ and $q = 1, 2, \ldots M$.
The following are the vectors A_p and C_p:

$$A_p = 2a \cdot r_p - a \tag{13}$$

$$C_p = 2a \cdot r_p \tag{14}$$

where A's components are progressively lowered from 2 to 0 throughout repetitions. r_p is the random vector in [0, 1]. Occasionally, the β and δ wolves participate in the hunting operation. Consequently, α, β, and δ will have a better idea of where the prey is. The top three solutions α, β, and δ have been saved, and the remaining agents must renovate their locations to resemble the best search agents' place.

$$D^i_{\alpha q} = |C_1 \cdot P^i_{\alpha q} - P^i_{pq}| \tag{15}$$

$$P^i_{1q} = P^i_{\alpha q} - A_1 D^i_{\alpha q} \tag{16}$$

$$D^i_{\beta q} = |C_1 \cdot P^i_{\beta q} - P^i_{pq}| \tag{17}$$

$$P^i_{2q} = P^i_{\beta q} - A_2 D^i_{\beta q} \tag{18}$$

$$D^i_{\delta q} = |C_1 \cdot P^i_{\delta q} - P^i_{pq}| \tag{19}$$

$$P^i_{3q} = P^i_{\delta q} - A_3 D^i_{\delta q} \tag{20}$$

$$P^{i+1}_{pq} = \frac{P^i_{1q} + P^i_{2q} + P^i_{3q}}{3} \tag{21}$$

When the target's movement comes to a halt, the grey wolves attack it, bringing the search to a close. Wolves reach the target when A's magnitude is smaller than 1, indicating an exploitation process. They split up to look for the prey and then converge in order to strike the target. To locate prey when A is more than one, the wolves must travel away from the target, which is called exploration. The exploration process is also aided by Vector C. The arbitrary value in [0, 2] is contained in vector C, as can be seen from equation 10. As a result, GWO may do more random operations throughout the optimization process to encourage exploration while avoiding local optima.
The conclusion is that the search process begins by randomly generating the grey wolf population. Throughout the iteration α, β, and δ approximate the target's predicted position. Each answer improves the distance between the prey and the predator. The exploitation and exploration were highlighted by the parameter 'a'. In situations where |A| is more than 1, solutions tend to move away from the target, while in situations where |A| is less than 1, solutions tend to congregate near the prey. The GWO comes to an end when a condition is satisfied at the conclusion. Fig. 2 depicts the GWO's process flow diagram, as indicated.

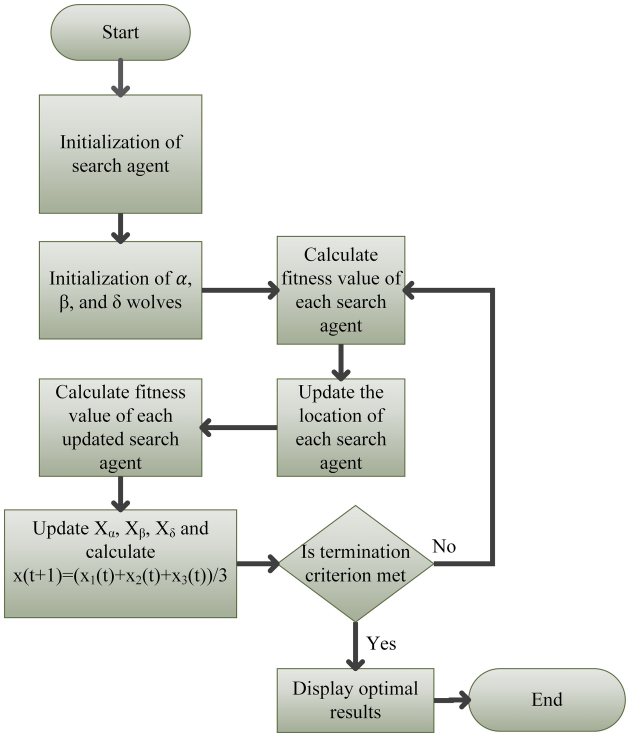

Figure 2. GWO process flow diagram.

4. Simulation experiment and results

It is evident that when the power system operates normally, it must ensure that its parameters don't exceed their limitations while simultaneously bearing its own load. However, when there is a rapid shift in the power system, it affects the system's parameters. It is necessary to make use of a controller in order to go around this obstacle.
Figure 1 depicts the model of a five-area power system with reheat turbine used in this investigation. As a secondary controller, each region employs a PID controller to provide an appropriate control signal. The controller is responsible for producing an error signal, which is then utilised by the power system. The MATLAB/Simulation tool was used to build the system that was under investigation. The power system being studied is being simulated by considering a load disturbance of one percent (0.01 p.u.) in area-1. The results of the simulation are obtained by operating the simulation for a total of thirty iterations. GWO is responsible for optimizing the gain values of the controller. The convergence of the cost curve with respect to the number of iterations for the GA, PSO, and GWO approaches is shown in Figure 3.
Each region has its own PID controller, which is tuned using GWO. The optimal values of the PID gains (Kp, Ki, Kd), which was obtained via GWO optimization, are:
For area-1 $K_{p1} = 6.1567$, $K_{i1} = 6.9693$, $K_{d1} = 9.0$;
For area-2 $K_{p2} = 0.5397$, $K_{i2} = 1.2030$, $K_{d2} = 3.5322$;
For area-3 $K_{p3} = 0.2197$, $K_{i3} = 0.3441$, $K_{d3} = 2.6715$;
For area-4 $K_{p4} = 0.0308$, $K_{i4} = 0.2964$, $K_{d4} = 0.7926$;
For area-5 $K_{p5} = 0.0622$, $K_{i5} = 0.0663$, $K_{d5} = 0.7448$.
Changes in frequency in all the five areas i.e. Δf_1, Δf_2, Δf_3, Δf_4, and Δf_5, and variations in the power flow through tie-line between all the five areas (ΔP_{tie1}, ΔP_{tie2}, ΔP_{tie3}, ΔP_{tie4}, ΔP_{tie5}) due to load change (0.01 p.u. MW) at time $t = 0$ obtained from the simulation experiment are displayed in Fig. 4 to Fig. 5, respectively.
The performance specifications obtained from Fig. 4 to Fig. 5 are summarized in Table 1, which includes the values for settling time for the tie-line power error and the frequency error, maximum undershoot, and maximum overshoot. The results obtained in [9] using GA, PSO, and FA technique are also given in Table 1 for comparison with

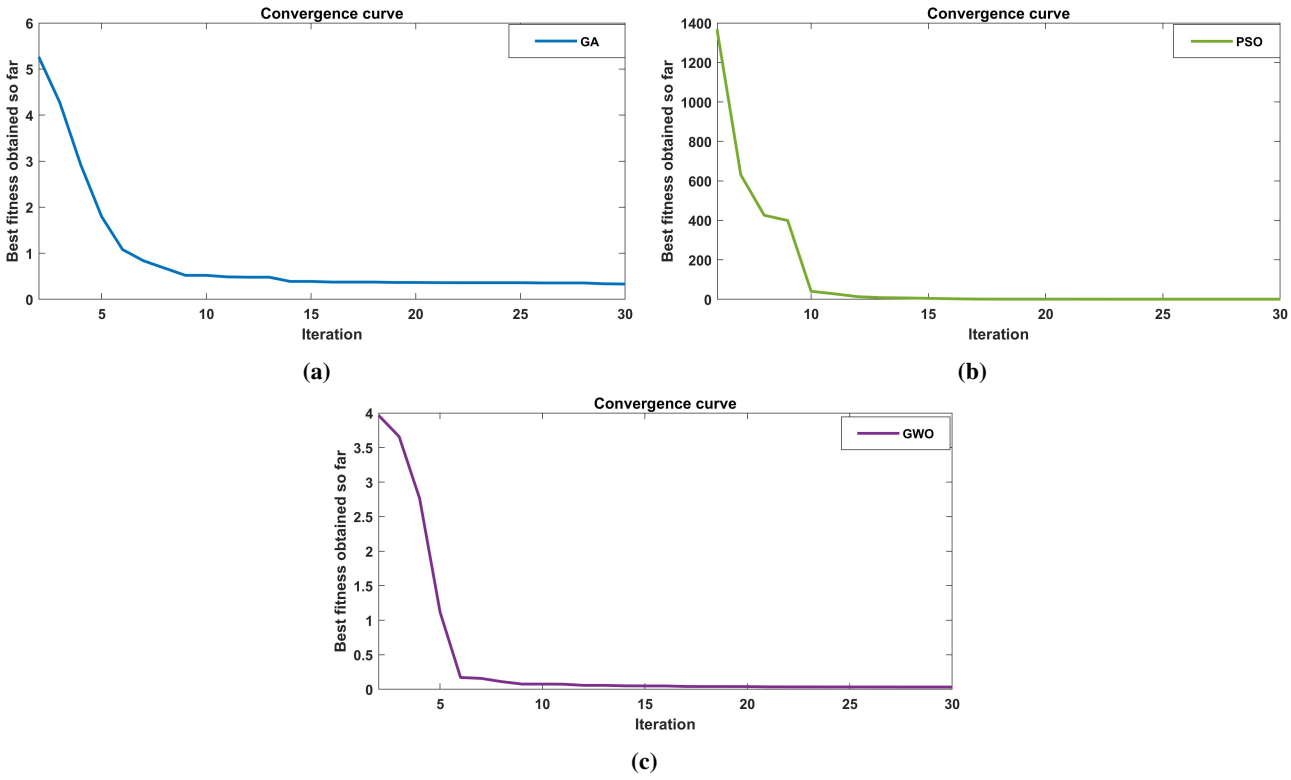

Figure 3. Convergence graph of cost curve with (a) GA, (b) PSO, and (c) GWO.

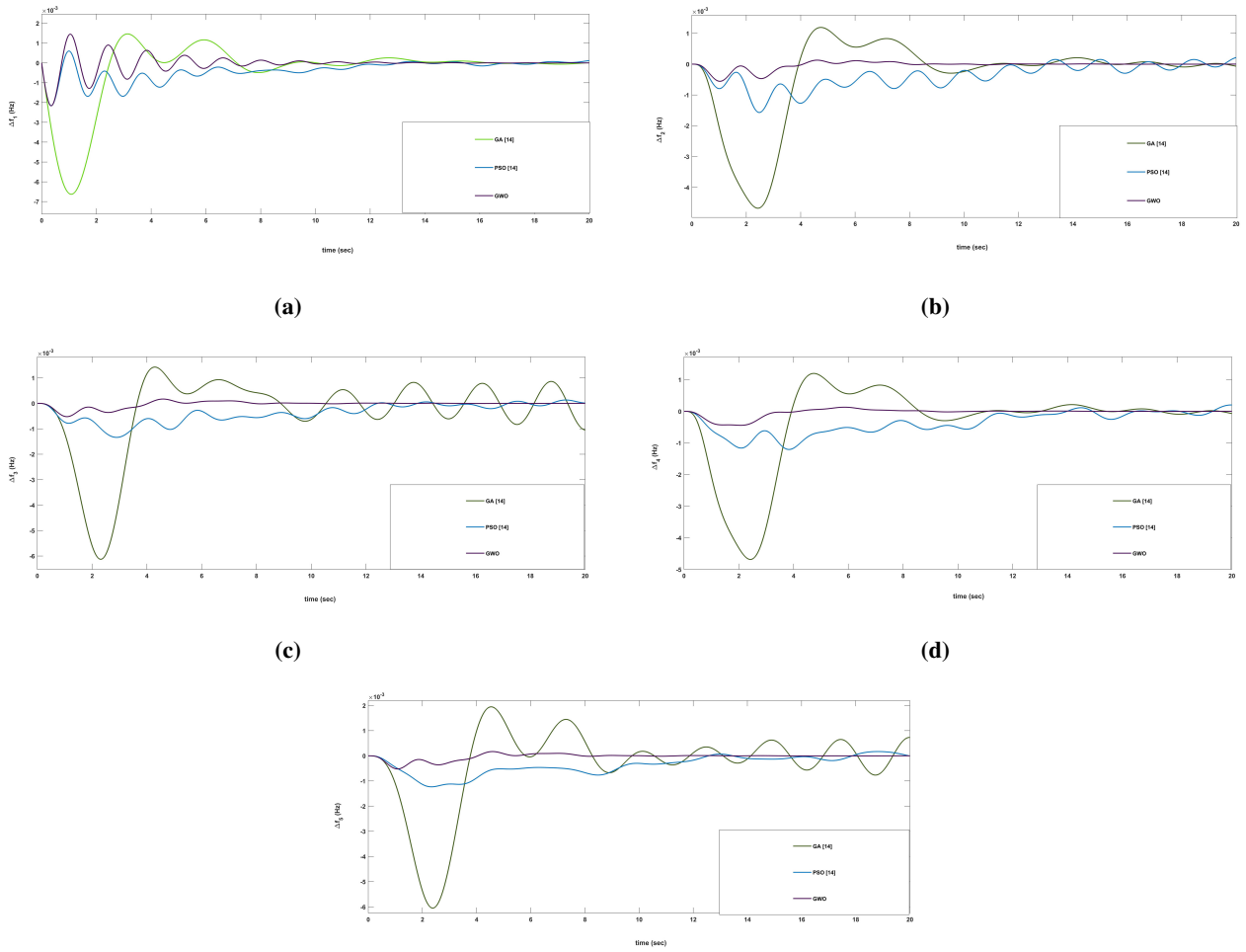

Figure 4. Frequency variations (a) in area-1, (b) in area-2 (c) in area-3 (d) in area-4 and (e) in area-5 due to load variations.

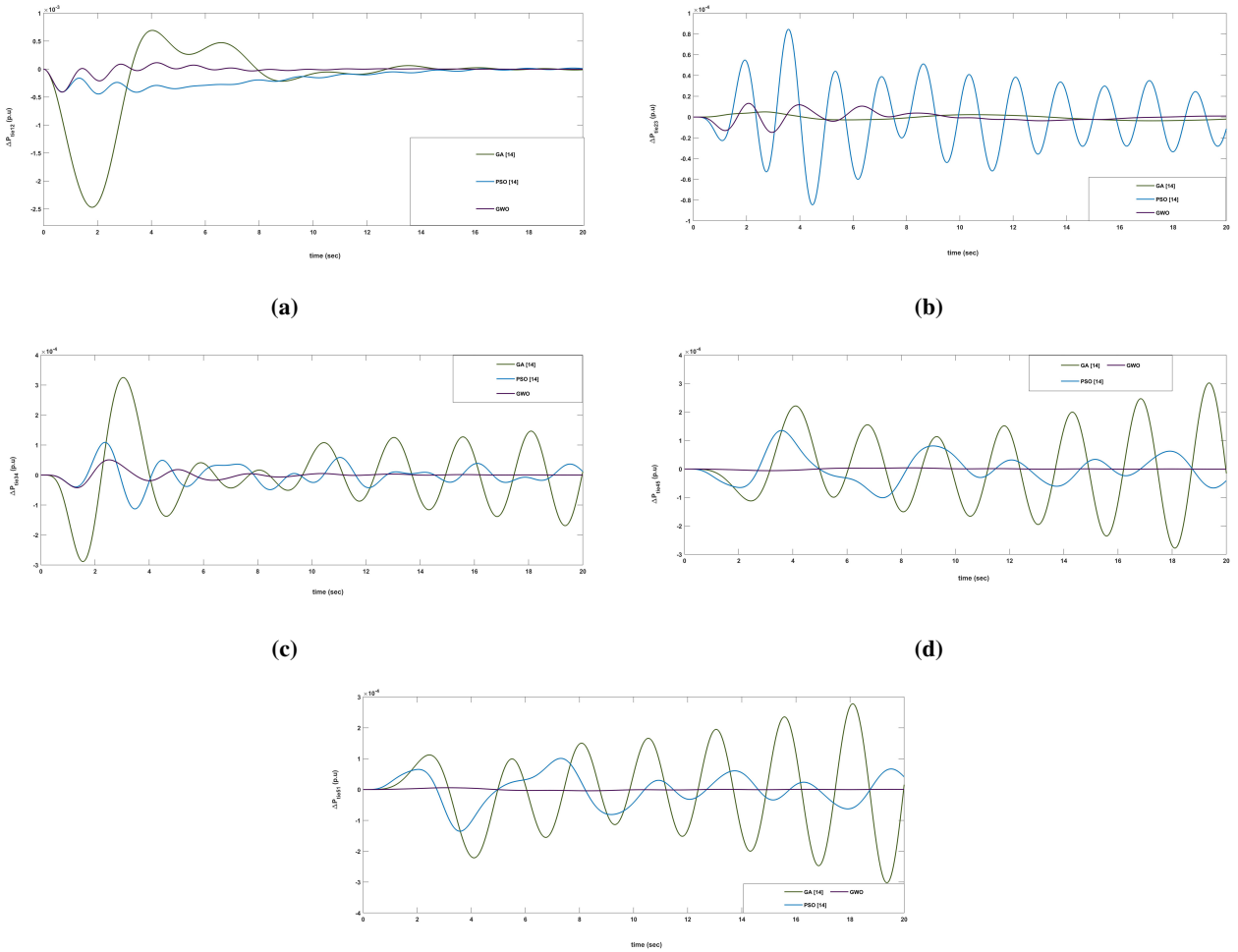

Figure 5. Tie-line power variations between (a) area-1 and area-2 (b) area-2 and area-3 (c) area-3 and area-4 (d) area-4 and area-5 and (e) area-5 and area-1.

Table 1. GWO-based PID controller's comparison.

		GA (PID) [9]	**PSO (PID) [9]**	**FFA (PID) [9]**	**GWO (PID)**
ITAE value		0.332	0.5067	–	0.0330
Settling Time	Δf_1	29.12	26.97	14.55	10.9798
	Δf_2	31.09	26.3	12.94	11.2026
	Δf_3	32.17	30.01	16.12	11.1371
	Δf_4	31.09	28.92	16.12	10.2207
	Δf_5	23.86	30.86	15.67	10.0759
	ΔP_{tie12}	25.83	34.83	24.53	10.6903
	ΔP_{tie23}	29.2	26.75	14.52	14.1311
	ΔP_{tie34}	24.76	24.59	24.05	16.0817
	ΔP_{tie45}	27.42	26.36	13.94	11.6628
	ΔP_{tie51}	23.25	27.70	24.05	12.6628
Peak Overshoot	Δf_1	0.0014	0.00059	0.0014	0.00145
	Δf_2	0.0011	0.00014	0.00029	0.000129
	Δf_3	0.0008	0.0012	0.00014	0.000129
	Δf_4	0.0011	0.00018	0.0005	0.000169
	Δf_5	0.0019	0.00016	0.00012	0.000169
	ΔP_{tie12}	0.0006	0.00001	0.0004	0.000114
	ΔP_{tie23}	0.000002	0.000084	0.00038	0.000013
	ΔP_{tie34}	0.0003	0.00015	0.0019	0.00005
	ΔP_{tie45}	0.0003	0.00044	0.00038	0.0000039
	ΔP_{tie51}	0.0003	0.000165	0.0019	0.0000058
Peak Undershoot (-ve)	Δf_1	0.0066	0.00217	0.011	0.00216
	Δf_2	0.0047	0.00156	0.0059	0.00055
	Δf_3	0.00612	0.00133	0.0052	0.000442
	Δf_4	0.0047	0.0011	0.0053	0.000522
	Δf_5	0.0060	0.00122	0.0056	0.000522
	ΔP_{tie12}	0.0025	0.0004	0.0078	0.00041
	ΔP_{tie23}	0.000004	0.000084	0.0059	0.0000148
	ΔP_{tie34}	0.0008	0.000165	0.00001	0.000042
	ΔP_{tie45}	0.0002	0.0001	0.0059	0.0000055
	ΔP_{tie51}	0.0002	0.00013	0.00017	0.0000039

other prevalent evolutionary optimization techniques.
For better understanding, the graphical depiction is presented in the form of a bar chart. It can be seen in Fig. 6 to Fig. 8. GWO demonstrates exceptional proficiency in addressing peak overshoot and undershoot, attaining enhancements spanning from 3.57 % to 99.91 % in comparison to GA, PSO, and FFA. This underscores its capability to sustain system stability with minimal oscillations. GWO optimized PID controller settles the frequency change for all the five areas and tie line power change between all areas to minimum value in less no. of iteration (30) as compared to FA (100), and give better result that can be verified from Fig. 6 to Fig. 9. When compared to the GA and the FA, the GWO algorithm displays considerable improvements in settling time across a variety of disturbance circumstances. These improvements range from 24.45 % to 35.05 % overall. In contrast, the settling time values for P_{tie23} (24.1311), P_{tie45} (29.6628), and P_{tie51} (29.6628) are greater for the case of the GWO-PID controller when compared to those of the other controllers. However, it is possible to overlook it when considering all of the other benefits GWO-PID has over other options.
Therefore, in contrast to the other methods that were investigated in [9], the GWO optimised controller provides a much superior response in terms of the settling times for changes in power flow through tie-line and frequency error, the overshoot value, and the undershoot value. Along with the load demand, other factors in the electrical network, such as turbine time constant, governor time constant, and so on, may also change; thus, to evaluate the reliable operation of GWO-PID, sensitivity analysis is given in the next section.

5. Robustness analysis

In this work, to test the resilience of the specified control mechanisms of the GWO-optimized PID controller, a robustness analysis is also undertaken by varying the system's parameters in a simulation experiment. Two cases of parameter uncertainty are undertaken for this analysis:

I. Case-1: change in turbine time constant (T_T) for $\pm 5\,\%$ and $\pm 10\,\%$.

II. Case-2: change in governor time constant (T_G) for $\pm 5\,\%$ and $\pm 10\,\%$.

The GWO-optimized PID gains values obtained in the previous sections under ideal conditions are considered for sensitivity analysis. The characteristics of the system are altered to induce uncertainty as a consequence of the aforementioned situations. For each of the two types of uncertainty, the PID gain value calculated from the nominal condition is chosen. For the aforesaid instances, Fig. 9 to 10 illustrate

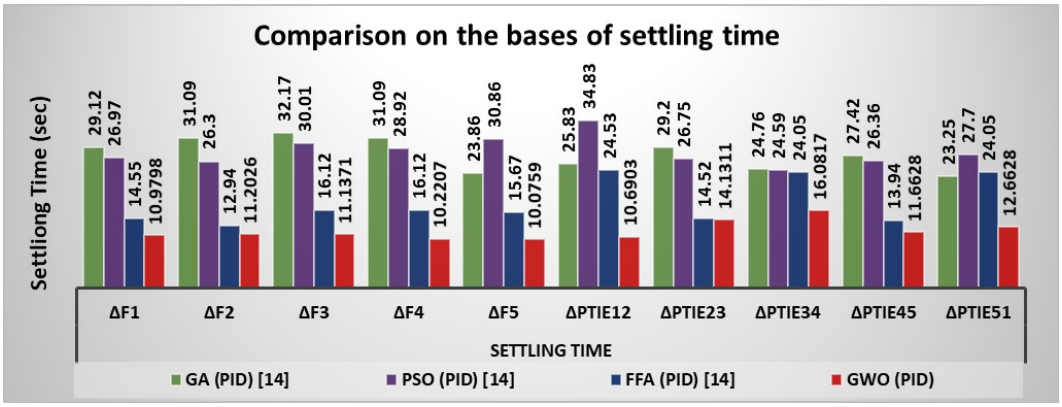

Figure 6. Comparison of settling time obtained.

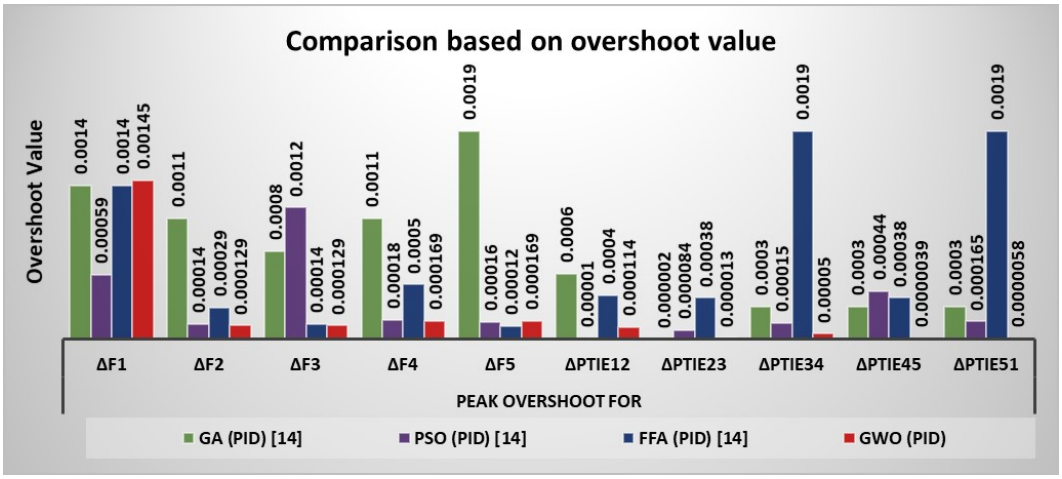

Figure 7. Comparison of GWO performance based on overshoot value.

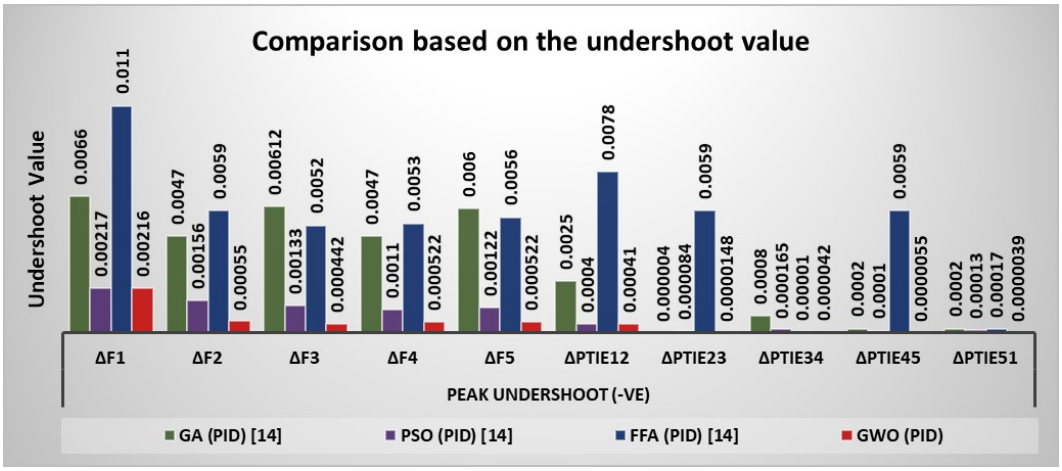

Figure 8. Comparison of GWO performance based on peak undershoot.

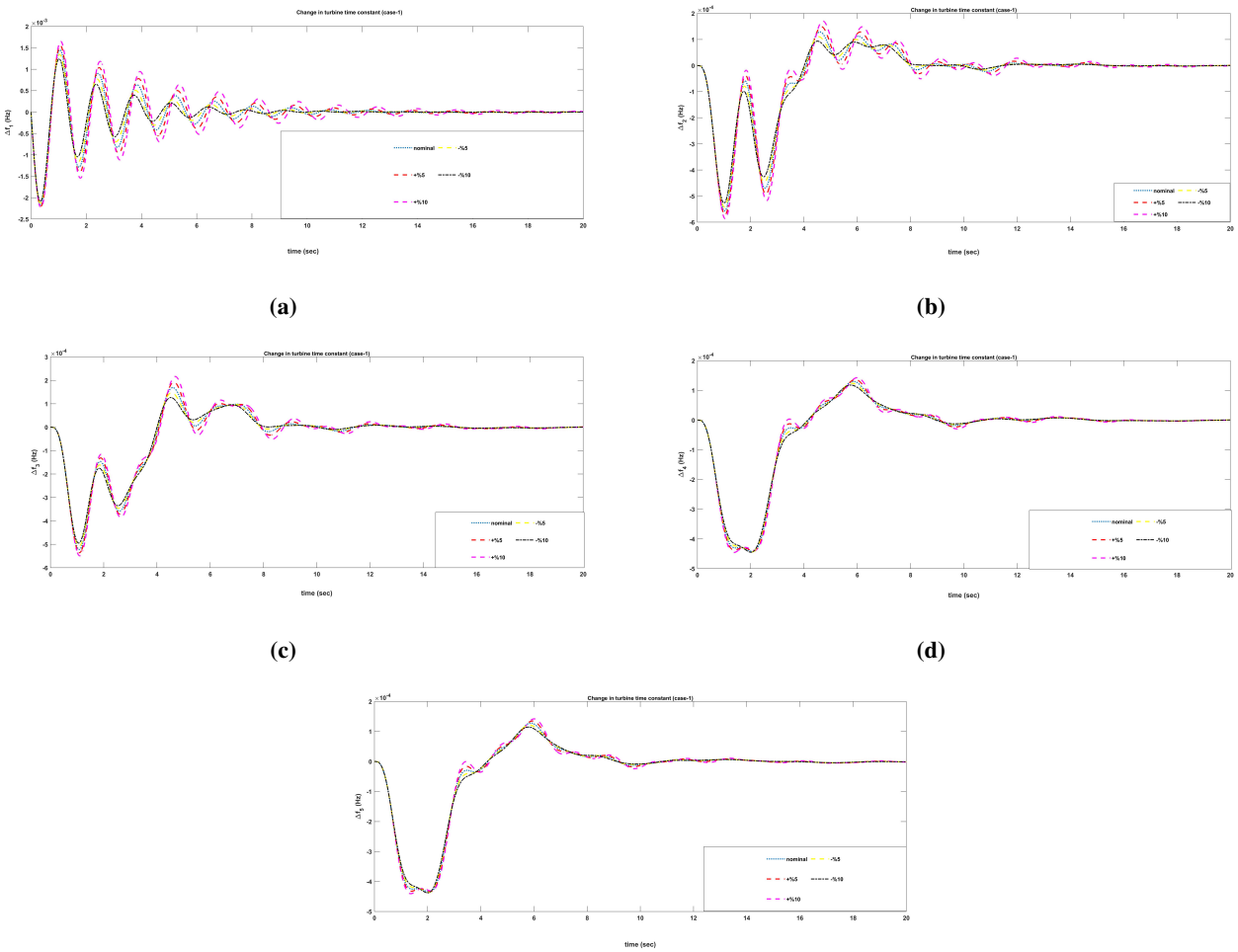

Figure 9. Frequency oscillations in area-1 to area-5 for case-1.

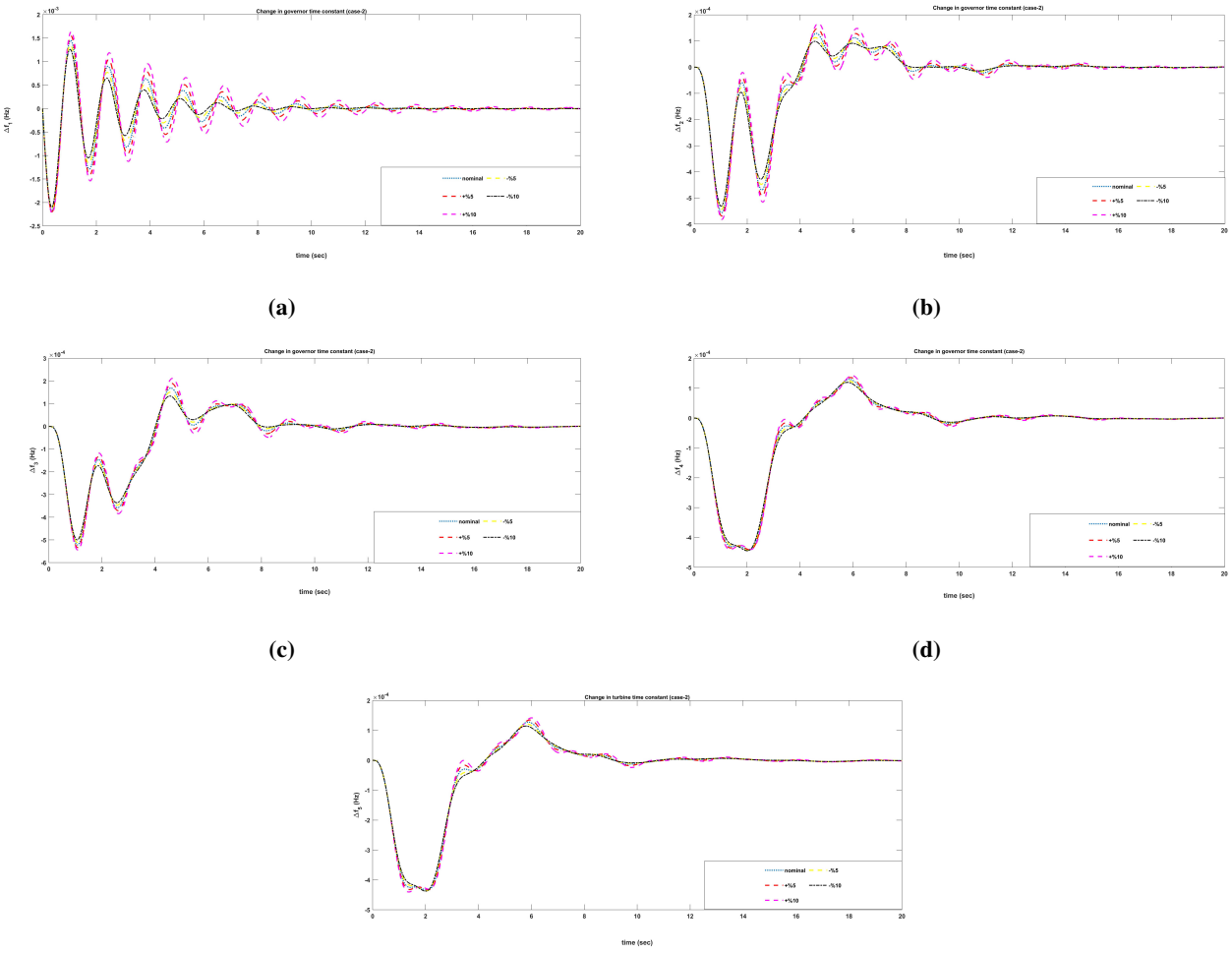

Figure 10. Frequency oscillation in area-1 to area-5 for case-2.

the frequency fluctuations in all the area. For case-1 of change in turbine time constant, the change in frequency for all the five areas are shown in Fig. 9(a) to 9(e).
Table 2 shows the system's performance for a 1 % change in load demand when various system parameters are changed. System parameter changes have little impact on overall system performance, as can be seen from the fact that the performance indices are essentially identical.
Figure 11 depicts the data from Table 2 in visual form. A look at the sensitivity study results of Fig. 9 and Fig. 11

Table 2. Robustness analysis under parameters uncertainties.

Parameter variation	**Percentage change**	***ITAE***	**Settling time for**				
			Δf_1	Δf_2	Δf_3	Δf_4	Δf_5
Nominal condition	0	0.0330	10.9798	11.2026	11.1371	10.1201	10.0759
Change in turbine time constant	For +5 %	0.0387	11.1946	12.1320	12.2212	10.2310	12.4168
	For +10 %	0.0420	13.2930	13.9822	14.0004	12.7529	13.6853
	For −5 %	0.0280	9.4902	11.0555	10.9611	10.2087	9.9615
	For −10 %	0.0253	7.9206	10.9008	7.8602	10.1574	8.8857
Change in governor time constant	For +5 %	0.0386	12.1399	12.0543	12.1329	10.1937	13.3298
	For +10 %	0.0416	13.1530	13.8608	14.87112	11.5909	13.5559
	For −5 %	0.0282	9.9536	11.1020	11.0125	10.2334	10.0514
	For −10 %	0.0256	7.9975	11.0003	10.8456	10.2029	9.9441

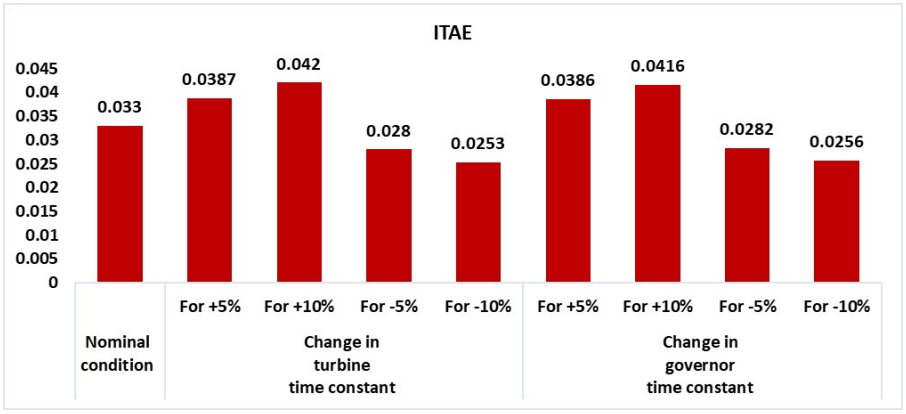

(a)

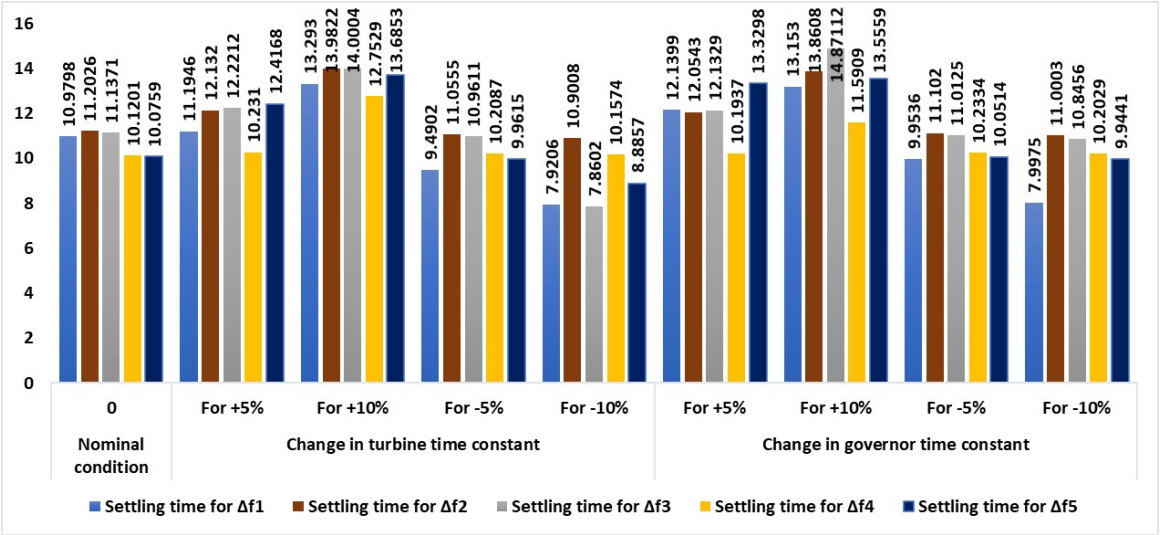

(b)

Figure 11. Comparison based on (a) *ITAE* value and (b) Settling time under the parameter's uncertainties.

shows that even with the introduction of uncertainties, the system's performance does not deviate much and stays close to its nominal value response. The preceding figures and bar graphs show that the overshoot value, undershoot value, settling time, and *ITAE* value only vary by a small amount. The settling time is almost the same in each scenario. This sensitivity study showed that even when parameters are variable, the controller still maintains its resilience.

6. Conclusion

The objective of the LFC is to maintain stability in the system's tie-line power as well as its frequency oscillations. Because of the increasing need for energy, having a reliable LFC system that can deal with the unpredictability of system parameters is more essential than ever. The study presented here uses GWO optimization methods to determine the optimized values for the gains of the PID controller that are used for the LFC of the Five-area power system. It has been determined that there was a step load shift in area-1 of 0.01 p.u., which was equivalent to one percent. Regarding the minimization of error-based performance indices, it has been noticed that the GWO-based PID controller used in LFC achieves a better performance than the GA, PSO, and FA-based PID controllers. In addition, the controller's robustness is examined in the presence of uncertainties in the system's parameters, such as turbine and governor time constant individually in the range of 10 percent for both systems. This is done in order to test the controller's ability to withstand these kinds of fluctuations. The results of the simulation show that the performance under unknown parameter conditions and under normal conditions are about equivalent. Additionally, the findings show that the settling time value for frequency error and tie-line power change falls within a range that is deemed acceptable. As a result, the GWO optimised PID parameters obtained at nominal levels are reliable and consistent and ensure robust performance even under the parameter's uncertainties.

Authors Contributions
All authors have contributed equally to prepare the paper.

Availability of Data and Materials
The data that support the findings of this study are available from the corresponding author upon reasonable request.

Conflict of Interests
The authors declare that they have no known competing financial interests or personal relationships that could have appeared to influence the work reported in this paper.

References

[1] A.J. Wood and B.F. Wollenberg. *"**Power Generation, Operation, and Control**."*. J. Wiley & Sons, 1996.

[2] O.I. Elgerd and C.E. Fosha. "**Optimum Megawatt-Frequency Control of Multiarea Electric Energy Systems**.". *IEEE Transactions on Power Apparatus and Systems*, PAS-89(4):556–563, 1970. DOI: https://doi.org/10.1109/TPAS.1970.292602.

[3] N. Ram Babu, S.K. Bhagat, L.C. Saikia, T. Chiranjeevi, R. Devarapalli, and F.P. García Márquez. "**A Comprehensive Review of Recent Strategies on Automatic Generation Control/Load Frequency Control in Power Systems**.". *Arch Computat Methods Eng*, 30(1):543–572, 2023. DOI: https://doi.org/10.1007/s11831-022-09810-y.

[4] S.K. Bhagat, N.R. Babu, L.C. Saikia, T. Chiranjeevi, R. Devarapalli, and F.P. García Márquez. "**A Review on Various Secondary Controllers and Optimization Techniques in Automatic Generation Control**.". *Arch Computat Methods Eng*, 30:3081–3111, 2023. DOI: https://doi.org/10.1007/s11831-023-09895-z.

[5] C. Ismayil, R. Sreerama Kumar, and T.K. Sindhu. "**Automatic generation control of single area thermal power system with fractional order PID ($PI^{\lambda}D^{\mu}$) controllers**.". *IFAC Proceedings Volumes*, 47(1):552–557, 2014. DOI: https://doi.org/10.3182/20140313-3-IN-3024.00025. 3rd International Conference on Advances in Control and Optimization of Dynamical Systems (2014).

[6] N. Saini and J. Ohri. "**Load Frequency Control of Multi-area Thermal Power System Using Grey Wolf Optimization**.". In S. Suhag, C. Mahanta, and S. Mishra, editors, *Control and Measurement Applications for Smart Grid*, page 347–357. Springer Nature Singapore, Singapore, 2022. DOI: https://doi.org/10.1007/978-981-16-7664-2_28.

[7] Y. Arya. "**Automatic generation control of two-area electrical power systems via optimal fuzzy classical controller**.". *J.*

Franklin Inst., 355(5):2662–2688, 2018. DOI: https://doi.org/10.1016/j.jfranklin.2018.02.004.

[8] R.K. Sahu, T.S. Gorripotu, and S. Panda. "**Automatic generation control of multi-area power systems with diverse energy sources using Teaching Learning Based Optimization algorithm**.". *Eng. Sci. Technol. an Int. J.*, 19(1):113–134, 2016. DOI: https://doi.org/10.1016/j.jestch.2015.07.011.

[9] K. Jagatheesan, B. Anand, S. Samanta, N. Dey, A.S. Ashour, and V.E. Balas. "**Design of a proportional-integral-derivative controller for an automatic generation control of multi-area power thermal systems using firefly algorithm**.". *IEEE/-CAA J. Autom. Sin.*, 6(2):503–515, 2019. DOI: https://doi.org/10.1109/JAS.2017.7510436.

[10] A. Bagheri, A. Jabbari, and S. Mobayen. "**An intelligent ABC-based terminal sliding mode controller for load-frequency control of islanded microgrids**.". *Sustain. Cities Soc.*, 64:102544, 2021. DOI: https://doi.org/10.1016/j.scs.2020.102544.

[11] J. Guo. "**Application of full order sliding mode control based on different areas power system with load frequency control**.". *ISA Trans.*, 92:23–34, 2019. DOI: https://doi.org/10.1016/j.isatra.2019.01.036.

[12] S. Prasad, S. Purwar, and N. Kishor. "**Load frequency regulation using observer based non-linear sliding mode control**.". *Int. J. Electr. Power Energy Syst.*, 104:178–193, 2019. DOI: https://doi.org/10.1016/j.ijepes.2018.06.035.

[13] V.A. Nishchitha and M. Pattnaik. "**Load Frequency Control of a Four-Area Interconnected Thermal-Hydro-Nuclear-Wind Power System with Non-Linearity using Fuzzy Logic PID Controller**.". *International Journal of Engineering Research & Technology (IJERT)*, 10(04):543–547, 2021. DOI: https://doi.org/10.17577/IJERTV10IS040319.

[14] P. Dash, L.C. Saikia, and N. Sinha. "**Automatic generation control of multi area thermal system using Bat algorithm optimized PD-PID cascade controller**.". *Int. J. Electr. Power Energy Syst.*, 68:364–372, 2015. DOI: https://doi.org/10.1016/j.ijepes.2014.12.063.

[15] H. Shabani, B. Vahidi, and M. Ebrahimpour. "**A robust PID controller based on imperialist competitive algorithm for load-frequency control of power systems**.". *ISA Trans.*, 52(1):88–95, 2013. DOI: https://doi.org/10.1016/j.isatra.2012.09.008.

[16] G. Magdy, G. Shabib, A.A. Elbaset, T. Kerdphol, Y. Qudaih, H. Bevrani, and Y. Mitani. "**Tustin's technique based digital decentralized load frequency control in a realistic multi power system considering wind farms and communications delays**.". *Ain Shams Eng. J.*, 10(2):327–341, 2019. DOI: https://doi.org/10.1016/j.asej.2019.01.004.

[17] R.K. Khadanga, A. Kumar, and S. Panda. "**A novel modified whale optimization algorithm for load frequency controller design of a two-area power system composing of PV grid and thermal generator**.". *Neural Computing and Applications*, 32(12):8205–8216, 2020. DOI: https://doi.org/10.1007/s00521-019-04321-7.

[18] A. Fathy and A.G. Alharbi. "**Recent Approach Based Movable Damped Wave Algorithm for Designing Fractional-Order PID Load Frequency Control Installed in Multi-Interconnected Plants with Renewable Energy**.". *IEEE Access*, 9:71072–71089, 2021. DOI: https://doi.org/10.1109/ACCESS.2021.3078825.

[19] A.M. Ersdal, L. Imsland, and K. Uhlen. "**Model Predictive Load-Frequency Control**.". *IEEE Trans. Power Syst.*, 31(1):777–785, 2016. DOI: https://doi.org/10.1109/TPWRS.2015.2412614.

[20] M. Elsisi, M.A.S. Aboelela, M. Soliman, and W. Mansour. "**Model Predictive Control of Two-Area Load Frequency Control Based Imperialist Competitive Algorithm**.". *TELKOMNIKA Indones. J. Electr. Eng.*, 16(1):75–82, 2015. DOI: https://doi.org/10.11591/telkomnika.v15i3.8856.

[21] J. Yang, X. Sun, K. Liao, J. Yang, Z. He, and L. Cai. "**Model predictive control-based load frequency control for power systems with wind-turbine generators**.". *IET Renew. Power Gener.*, 13(15):2871–2879, 2019. DOI: https://doi.org/10.1049/iet-rpg.2018.6179.

[22] N.R. Babu and L.C. Saikia. "**Automatic generation control of a solar thermal and dish-stirling solar thermal system integrated multi-area system incorporating accurate HVDC link model using crow search algorithm optimised FOPI Minus FODF controller**.". *IET Renew. Power Gener.*, 13(12): 2221–2231, 2019. DOI: https://doi.org/10.1049/iet-rpg.2018.6089.

[23] A. Dokht Shakibjoo, M. Moradzadeh, S.Z. Moussavi, A. Mohammadzadeh, and L. Vandevelde. "**Load frequency control for multi-area power systems: A new type-2 fuzzy approach based on Levenberg–Marquardt algorithm**.". *ISA Trans.*, 121:40–52, 2022. DOI: https://doi.org/10.1016/j.isatra.2021.03.044.

[24] A. Demiroren and H.L. Zeynelgil. "**GA application to optimization of AGC in three-area power system after deregulation**.". *Int. J. Electr. Power Energy Syst.*, 29(3):230–240, 2007. DOI: https://doi.org/10.1016/j.ijepes.2006.07.005.

[25] S.K. Sinha, R.N. Patel, and R. Prasad. "**Application of GA and PSO Tuned Fuzzy Controller for AGC of Three Area Thermal- Thermal-Hydro Power System**.". *Int. J. Comput. Theory Eng.*, 2(2):1793–8201, 2010. DOI: https://doi.org/10.7763/IJCTE.2010.V2.146.

[26] S.S. Dhillon, J.S. Lather, and S. Marwaha. "**Multi Area Load Frequency Control Using Particle Swarm Optimization and Fuzzy Rules**.". *in Procedia Computer Science, Elsevier*, 57:460–472, 2015. DOI: https://doi.org/10.1016/j.procs.2015.07.363.

[27] N.K. Bahgaat, M.I. El-Sayed, M.A.M. Hassan, and F.A. Bendary. "**Load Frequency Control in Power System via Improving PID Controller Based on Particle Swarm Optimization and ANFIS Techniques**.". *Int. J. Syst. Dyn. Appl.*, 3(3):1–24, 2014. DOI: https://doi.org/10.4018/ijsda.2014070101.

[28] N. Saini and J. Ohri. "**Optimal Load Frequency Control of a Multi-Area Power System with Dead Band Effect and Generation Rate Constraints**.". *Majlesi J. Electr. Eng.*, 17(1), 2023. DOI: https://doi.org/10.30486/mjee.2023.1970197.0.

[29] N.R. Babu and L.C. Saikia. "**Optimal location of accurate HVDC and energy storage devices in a deregulated AGC integrated with PWTS considering HPA-ISE as performance index**.". *Eng. Sci. Technol. an Int. J.*, 33:101072, 2022. DOI: https://doi.org/10.1016/j.jestch.2021.10.004.

[30] M. Raju, L.C. Saikia, and N. Sinha. "**Automatic generation control of a multi-area system using ant lion optimizer algorithm based PID plus second order derivative controller**.". *Int. J. Electr. Power Energy Syst.*, 80:52–63, 2016. DOI: https://doi.org/10.1016/j.ijepes.2016.01.037.

[31] E. Çelik, N. Öztürk, and E.H. Houssein. "**Influence of energy storage device on load frequency control of an interconnected dual-area thermal and solar photovoltaic power system**.". *Neural Comput. Appl.*, 34:20083–20099, 2022. DOI: https://doi.org/10.1007/s00521-022-07558-x.

[32] K. Naidu, H. Mokhlis, and A.H.A. Bakar. "**Multiobjective optimization using weighted sum Artificial Bee Colony algorithm for Load Frequency Control**.". *Int. J. Electr. Power Energy Syst.*, 55:657–667, 2014. DOI: https://doi.org/10.1016/j.ijepes.2013.10.022.

[33] N. Saini and J. Ohri. "**Load frequency control in three-area single unit power system considering non-linearities effect**.". *Cybern. Phys.*, 12(1):60–69, 2023. DOI: https://doi.org/10.35470/2226-4116-2023-12-1-60-69.